Extracellular matrix protein Matrilin-4 regulates stress-induced HSC proliferation via CXCR4

Hannah Uckelmann,[1,2] Sandra Blaszkiewicz,[1,2]* Claudia Nicolae,[3]* Simon Haas,[1,2] Alexandra Schnell,[1,2] Stephan Wurzer,[1,2] Raimund Wagener,[4] Attila Aszodi,[3,5] and Marieke Alida Gertruda Essers[1,2]

[1]HSCs and Stress Group, Division of Stem Cells and Cancer, German Cancer Research Center (DKFZ), 69121 Heidelberg, Germany
[2]Heidelberg Institute for Stem Cell Technologies and Experimental Medicine gGmbH, 69120 Heidelberg, Germany
[3]Department of Molecular Medicine, Max Planck Institute for Biochemistry, 82152 Planegg, Germany
[4]Center for Biochemistry, Medical Faculty and Center for Molecular Medicine (CMMC), University of Cologne, 50931 Cologne, Germany
[5]Department of General, Trauma, Hand, and Plastic Surgery, Ludwig-Maximilians University, 80539 Munich, Germany

During homeostasis, hematopoietic stem cells (HSCs) are mostly kept in quiescence with only minor contribution to steady-state hematopoiesis. However, in stress situations such as infection, chemotherapy, or transplantation, HSCs are forced to proliferate and rapidly regenerate compromised hematopoietic cells. Little is known about the processes regulating this stress-induced proliferation and expansion of HSCs and progenitors. In this study, we identified the extracellular matrix (ECM) adaptor protein Matrilin-4 (Matn4) as an important negative regulator of the HSC stress response. Matn4 is highly expressed in long-term HSCs; however, it is not required for HSC maintenance under homeostasis. In contrast, Matn4 is strongly down-regulated in HSCs in response to proliferative stress, and Matn4 deficiency results in increased proliferation and expansion of HSCs and progenitors after myelosuppressive chemotherapy, inflammatory stress, and transplantation. This enhanced proliferation is mediated by a transient down-regulation of CXCR4 in $Matn4^{-/-}$ HSCs upon stress, allowing for a more efficient expansion of HSCs. Thus, we have uncovered a novel link between the ECM protein Matn4 and cytokine receptor CXCR4 involved in the regulation of HSC proliferation and expansion under acute stress.

INTRODUCTION

The life-long blood supply is maintained by a pool of self-renewing, multipotent hematopoietic stem cells (HSCs), which are found in a quiescent state for most of their life (Orkin and Zon, 2008). In acute stress situations such as infection, chemotherapy, and transplantation, proinflammatory cytokines such as IFN-α act as an emergency signal to recruit quiescent HSCs into an active cell cycle to replenish the compromised blood supply (Essers et al., 2009; Baldridge et al., 2010). However, the underlying molecular mechanisms for this are poorly understood.

HSC quiescence is tightly regulated by paracrine and autocrine signals and direct interactions within the BM niche (Scadden, 2014). Cell surface receptors such as c-Kit, N-cadherin, or integrins mediate direct adhesion of HSCs to niche cells or their surrounding extracellular matrix (ECM; Ellis and Tanentzapf, 2010). Additionally, cytokines produced by niche cells such as TGF-β, stem cell factor, and CXCL12

induce HSC quiescence and BM retention (Heissig et al., 2002; Katayama et al., 2006; Itkin and Lapidot, 2011). The CXCL12–CXCR4 axis for instance is central in regulating HSC migration and homing to the BM niche and, in contrast, promoting HSC quiescence by inducing the expression of cell cycle inhibitors (Sugiyama et al., 2006; Nie et al., 2008; Tzeng et al., 2011).

The BM ECM surrounding HSCs is composed of proteoglycans, collagens, and noncollagenous proteins and can affect adhesion, migration, and proliferation of HSCs (Klein, 1995; Ellis and Tanentzapf, 2010). Matrilins (Matns) comprise a family of oligomeric ECM adaptor proteins that connect these different ECM components, forming a supramolecular structure (Deák et al., 1999; Klatt et al., 2001). Matn1 and 3 are mainly expressed in skeletal tissue, whereas Matn2 and 4 show a broad expression pattern (Klatt et al., 2011). Matn1, 2, and 3 have been shown to directly interact with integrins and activate several intracellular signaling pathways; however, the molecular mechanism of this signaling remains unresolved (Mann et al., 2007).

Here, we show that Matn4 is highly expressed in quiescent HSCs, and expression decreases during proliferative

---

*S. Blaszkiewicz and C. Nicolae contributed equally to this paper.

Correspondence to Marieke Alida Gertruda Essers: m.essers@dkfz.de

H. Uckelmann's present address is Center for Epigenetics Research, Memorial Sloan-Kettering Cancer Center, New York, NY 10065.

C. Nicolae's present address is Dept. of Biochemistry and Molecular Biology, The Pennsylvania State University College of Medicine, Hershey, PA 17033.

Abbreviations used: 5-FU, 5-fluorouracil; ECM, extracellular matrix; ES, embryonic stem; HSC, hematopoietic stem cell; LT-HSC, long-term HSC; PB, peripheral blood; pI:C, polyinosinic:polycytidylic acid; qRT-PCR, quantitative real-time PCR; WBC, white blood cell.

stress, permitting the activation and expansion of HSCs. Intriguingly, HSCs lacking Matn4 respond more effectively to stress and show a robust competitive transplantation advantage, mediated by down-regulation of CXCR4 expression in Matn4-deficient HSCs in stress situations. In summary, our data suggest that high expression of Matn4 in HSCs confers a resistance to stress stimuli. In situations of acute stress such as infection or transplantation however, this protection is rapidly lost to allow HSCs to efficiently replenish the blood system.

RESULTS AND DISCUSSION
Matn4 is highly expressed in HSCs but dispensable for steady-state hematopoiesis

The ECM surrounding HSCs in the BM is poorly described. Gene expression analysis revealed that the ECM protein Matn4 is highly expressed in long-term HSCs (LT-HSCs) and severely down-regulated upon differentiation to short-term HSCs and multipotent progenitor cells (Fig. 1 A). Matn1, Matn2, and Matn3 were only low expressed in stem and progenitor cells with no enrichment in HSCs (Fig. 1 A). To examine the role of Matn4 in normal hematopoiesis, mice lacking Matn4 ($Matn4^{-/-}$) were generated. Previous studies using single or double KO models of Matns revealed functional redundancy in this protein family (Aszódi et al., 1999; Mátés et al., 2004; Nicolae et al., 2007). Therefore, quadruple KO mice lacking all four family members ($Matn1-4^{-/-}$) were established from single mutant lines. $Matn4^{-/-}$ and $Matn1-4^{-/-}$ mice were viable, fertile, had a normal life span, and showed no apparent gross abnormalities. Whereas both $Matn4^{-/-}$ and $Matn-1-4^{-/-}$ mice presented with decreased Lin$^-$Sca-1$^+$cKit$^+$ (LSK) numbers, their LT-HSC numbers were comparable with WT C57BL/6 mice (Fig. 1, B and C). Both KO models generated normal amounts of myeloid and lymphoid lineages with only minor differences in T cells and granulocytes (Fig. 1 D). Cell cycle analysis revealed comparable numbers of quiescent HSCs (Fig. 1, E and F). In addition, in $Matn4^{-/-}$, mice the lack of Matn4 is not compensated by increased expression of the other Matns (Fig. 1 G). Thus, under homeostasis, Matn4 is not required for the maintenance of normal hematopoiesis and HSC quiescence.

Proliferative stress induces the down-regulation of Matn4 in HSCs

Matn4 expression is highest in the most quiescent HSCs and anticorrelates with increasing proliferative activity from HSCs to progenitors. To test whether Matn4 transcript levels were also down-regulated when HSCs are forced to proliferate, different stress conditions were tested. Interestingly, gene expression profiling revealed Matn4 as the most down-regulated gene in HSCs isolated from IFN-α–treated mice (Fig. 2 A), which could be confirmed on the protein level in HSCs isolated from mice treated with polyinosinic:polycytidylic acid (pI:C), inducing a strong IFN-α response (Fig. 2, B and C). In contrast, Matn4 down-regulation was abolished in HSCs isolated from $Ifnar^{-/-}$ and $Stat1^{-/-}$ mice,

demonstrating that Matn4 expression levels in HSCs are controlled by Ifnar–Stat1 signaling (Fig. 2 D). In addition, treatment of mice with LPS, transplantation, irradiation, or in vitro culture of HSCs also led to a significant decline in Matn4 levels in HSCs (Fig. 2 E). Collectively, these data indicate that stress-induced proliferation of HSCs is accompanied by a strong down-regulation of Matn4 in HSCs.

Loss of Matn4 leads to an increased HSC proliferation in response to stress

To test whether there is a functional link between the down-regulation of Matn4 and the activation of HSCs by IFN-α, HSC proliferation and blood recovery of WT and $Matn1-4^{-/-}$ mice were measured. pI:C treatment resulted in increased cell cycle entry of $Matn1-4^{-/-}$ HSCs compared with WT HSCs (Fig. 3 A), accompanied by a higher white blood cell (WBC) and platelet count during recovery (Fig. 3, B and C). To evaluate whether $Matn1-4^{-/-}$ showed improved recovery in other stress situations, mice were treated with the chemotherapeutic 5-fluorouracil (5-FU). As observed after pI:C treatment, $Matn1-4^{-/-}$ HSCs proliferated more in response to 5-FU (Fig. 3 D) and showed more rapid recovery of WBCs and platelets (Fig. 3, E and F). Similar phenotypes were observed in $Matn4^{-/-}$ mice (not depicted). Despite their enhanced proliferative response, $Matn1-4^{-/-}$ HSCs returned to quiescence at the same time as WT HSCs after pI:C and 5-FU treatment (Fig. 3, A–D). This was further supported by serial 5-FU treatments, where HSCs were repeatedly stressed just after recovery leading to their exhaustion and pancytopenia. There was no difference in the survival curves of WT and $Matn1-4^{-/-}$ mice upon serial 5-FU treatment, further supporting our hypothesis that $Matn1-4^{-/-}$ HSCs return to quiescence efficiently and to the same extent as WT HSCs, even after serial rounds of stress (Fig. 3 G).

Matn4 limits the expansion of HSCs and progenitors

Strikingly, both LSK as well as LT-HSC numbers were dramatically increased on day 9 after 5-FU treatment (Fig. 3, H and I; and Fig. S1). To show that this massive expansion is not caused by contamination of the HSC gate, we performed a CFU assay with equal numbers of sorted $Matn1-4^{-/-}$ and WT LSKs. Remarkably, $Matn1-4^{-/-}$ LSKs showed a higher colony-forming potential than WT LSKs, suggesting an increase in functional HSCs and progenitors (Fig. 3 J). In agreement with this, untreated $Matn1-4^{-/-}$ LSK cells also showed higher CFUs than WT cells with larger and more colonies, which was even more pronounced in secondary CFUs (Fig. 3 K). The increased colony size could be rescued by the addition of recombinant Matn4 to the CFU medium (Fig. 3 L). Additionally, WT colony size was significantly reduced upon addition of recombinant Matn4, suggesting that Matn4 generally exerts growth inhibitory effects on HSCs. Collectively, these data show that in the absence of Matn4, HSCs proliferate and expand more efficiently in response to stress, resulting in more rapid reestablishment of homeostatic blood levels.
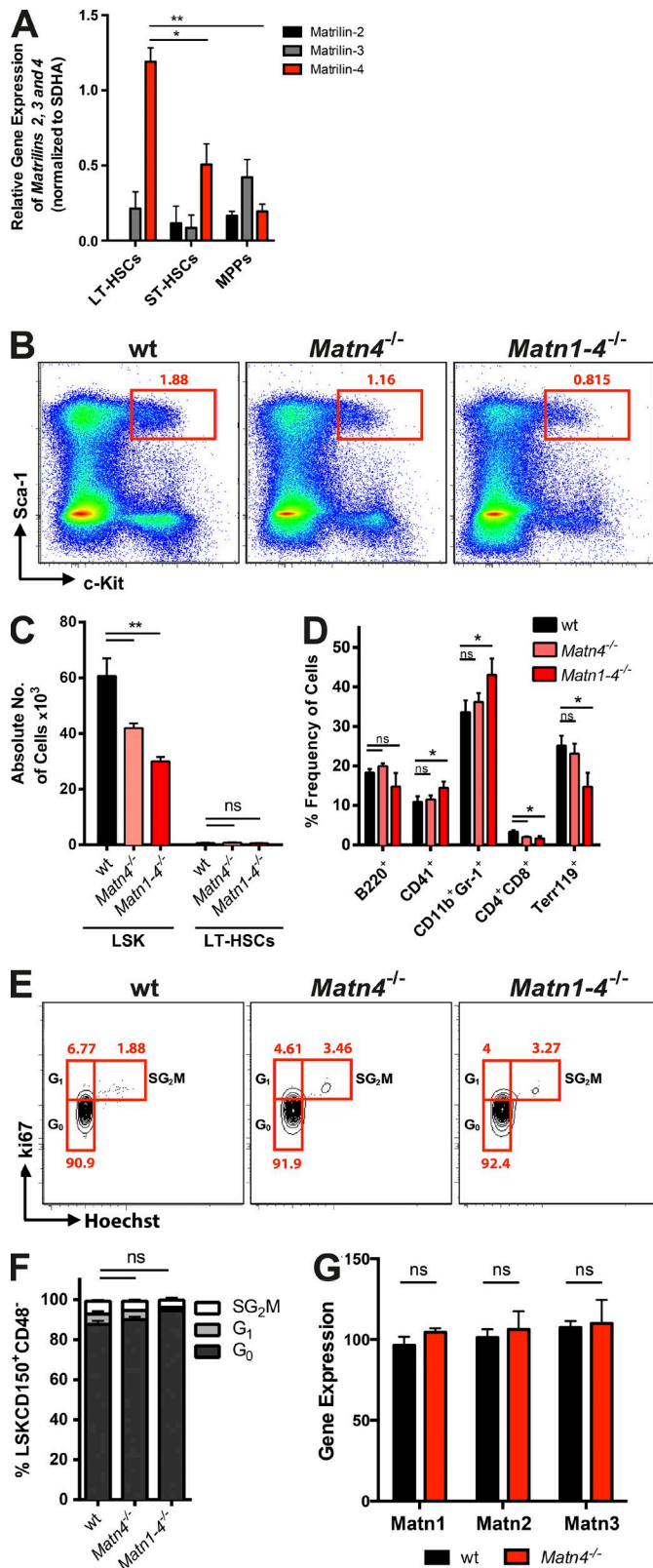
Figure 1. **Matn4 is highly expressed in HSCs but dispensable for steady–state hematopoiesis.** (A) Matn2, 3, and 4 mRNA expression in LT-HSCs (Lin⁻Sca-1⁺c-Kit⁺CD150⁺CD48⁻CD34⁻), short term HSCs (ST-HSCs; Lin⁻Sca-1⁺c-Kit⁺CD150⁺CD48⁻CD34⁺), and multipotent progenitors (MPPs; Lin⁻Sca-1⁺c-Kit⁺CD150⁺CD48⁺) of WT mice. (B) Representative LSK FACS plots showing percentage of LSK in WT, *Matn4⁻/⁻*, and *Matn1–4⁻/⁻* mice. (C) Absolute numbers of LSK and LSKCD150⁺CD48⁻ of WT, *Matn4⁻/⁻*, and *Matn1–4⁻/⁻* mice determined by FACS and normalized to the total BM cell counts per femur. (D) Frequency of B cells (B220⁺), megakaryocytes (CD41⁺), granulocytes (CD11b⁺Gr-1⁺), T cells (CD4⁺CD8⁺), and erythrocytes (Terr119⁺) in BM of WT, *Matn4⁻/⁻*, and *Matn1–4⁻/⁻* mice determined by FACS. (E and F) Representative FACS plots (E) and quantification (F) of cell cycle distribution (Ki67/Hoechst) of WT, *Matn4⁻/⁻*, and *Matn1–4⁻/⁻* HSCs (LSKCD150⁺CD48⁻). (G) Matn1, 2, and 3 mRNA expression levels of HSCs (LSKCD150⁺CD48⁻) isolated from WT and Matn4⁻/⁻ mice isolated 4 wk after transplantation, derived from microarray analysis. $n = 3$ mice/group. Unpaired Student's *t* test analysis was performed on three independent experiments. *, P < 0.05; **, P < 0.01. Data are mean ± SEM.
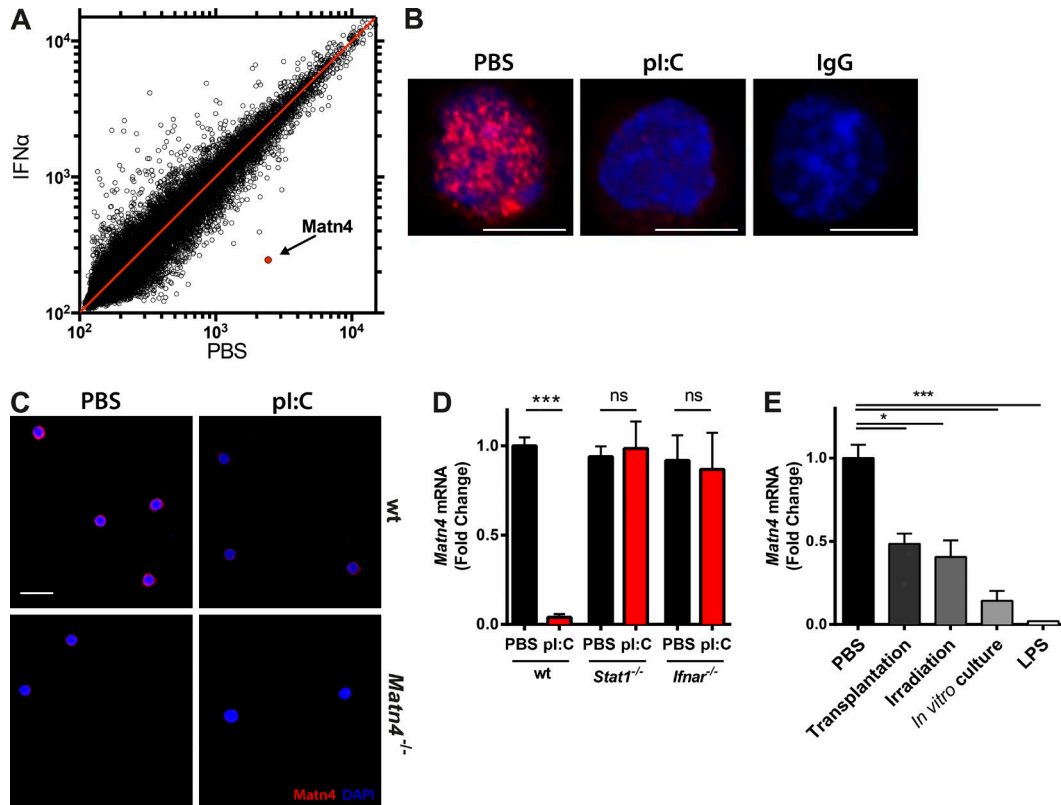
Figure 2. **Proliferative stress is associated with Matn4 down-regulation in HSCs.** (A) Scatterplot of changes in mRNA expression levels of HSCs (LKCD150⁺CD48⁻) isolated from triplicate PBS- or IFN-α–treated WT mice (5 × 10⁶ U/kg for 16 h), derived from microarray analysis. Matn4 is marked in red. (B) Representative immunofluorescence images of LT-HSCs (LSKCD150⁺CD48⁻CD34⁻) from WT mice treated with PBS or pI:C (5 mg/kg for 16 h), stained for Matn4 (red) and DAPI (blue). Bars, 5 µm. (C) Immunofluorescence images of LT-HSCs (LSKCD150⁺CD48⁻CD34⁻) from WT and Matn4⁻/⁻ mice treated with PBS or pI:C (5 mg/kg for 16 h), stained for Matn4 (red) and DAPI (blue). n = 3. Bar, 20 µm. Representative images are from three independent experiments. (D) Fold change of Matn4 mRNA expression validated by qRT-PCR of sorted HSCs (LKCD150⁺CD48⁻) from PBS- or pI:C (5 mg/kg for 16 h)-treated WT, Stat1⁻/⁻, and Ifnar⁻/⁻ mice. (E) Matn4 mRNA levels determined by qRT-PCR of WT HSCs (LSKCD150⁺CD48⁻) isolated 24 h after transplant, irradiation (2 × 500 Rad), or in vitro culture and LKCD150⁺CD48⁻ HSCs after LPS (0.25 mg/kg for 24 h) treatment. (A, B, D, and E) n = 3 mice/group. (D and E) Unpaired Student's t test analysis was performed on three independent experiments. *, P < 0.05; ***, P < 0.001. Data are mean ± SEM.

To further characterize this, single Matn4⁻/⁻ HSCs were kept in liquid cultured for 7 d, and cell numbers and type of colonies were quantified. Matn4⁻/⁻ HSCs produced larger colonies with a higher percentage of undifferentiated and mixed colonies (Fig. 3, M–P). Of note, a few days later, undifferentiated colonies started to generate mixed colonies (not depicted), suggesting that Matn4⁻/⁻ HSCs initially self-renew more before differentiating into larger colonies. The increase in undifferentiated colonies could be rescued by adding recombinant Matn4 to the culture medium, supporting the hypothesis that Matn4 limits the expansion of HSCs (Fig. 3, O and P).

Matn4⁻/⁻ HSCs show increased competitive repopulation capacity in BM transplantations

After transplantation into a lethally irradiated recipient, donor cells are confronted with an excess of inflammatory cytokines generated within the irradiated BM niche (Xun et al., 1994). To reestablish the hematopoietic system, a massive expansion of donor HSCs and progenitors is required. To examine whether loss of Matn4 could enhance this expansion of HSCs upon transplantation, competitive BM repopulation assays were performed by mixing equal amounts of Matn4⁻/⁻ or Matn1–4⁻/⁻ BM cells with WT CD45.1 competitor BM cells (50:50%; Fig. 4 A). Only 4 wk after transplantation, Matn4⁻/⁻ and Matn1–4⁻/⁻ cells comprised >80% of the blood granulocyte chimerism (Fig. 4 A). This competitive advantage was sustained over time, and Matn4⁻/⁻ and Matn1–4⁻/⁻ BM cells outcompeted WT CD45.1 cells across all differentiated lineages, up to HSCs (Fig. 4 B). In secondary competitive transplantations, Matn1–4⁻/⁻ cells again rapidly showed improved reconstitution (>80%; Fig. 4 C). Limiting dilution assays confirmed that the improved reconstitution capacity was not because of an increased number of functional HSCs but rather a proliferative advantage of Matn4⁻/⁻ cells (Fig. 4 D).

Increased proliferative stress often leads to premature exhaustion of HSCs (Sato et al., 2009; Walter et al., 2015).
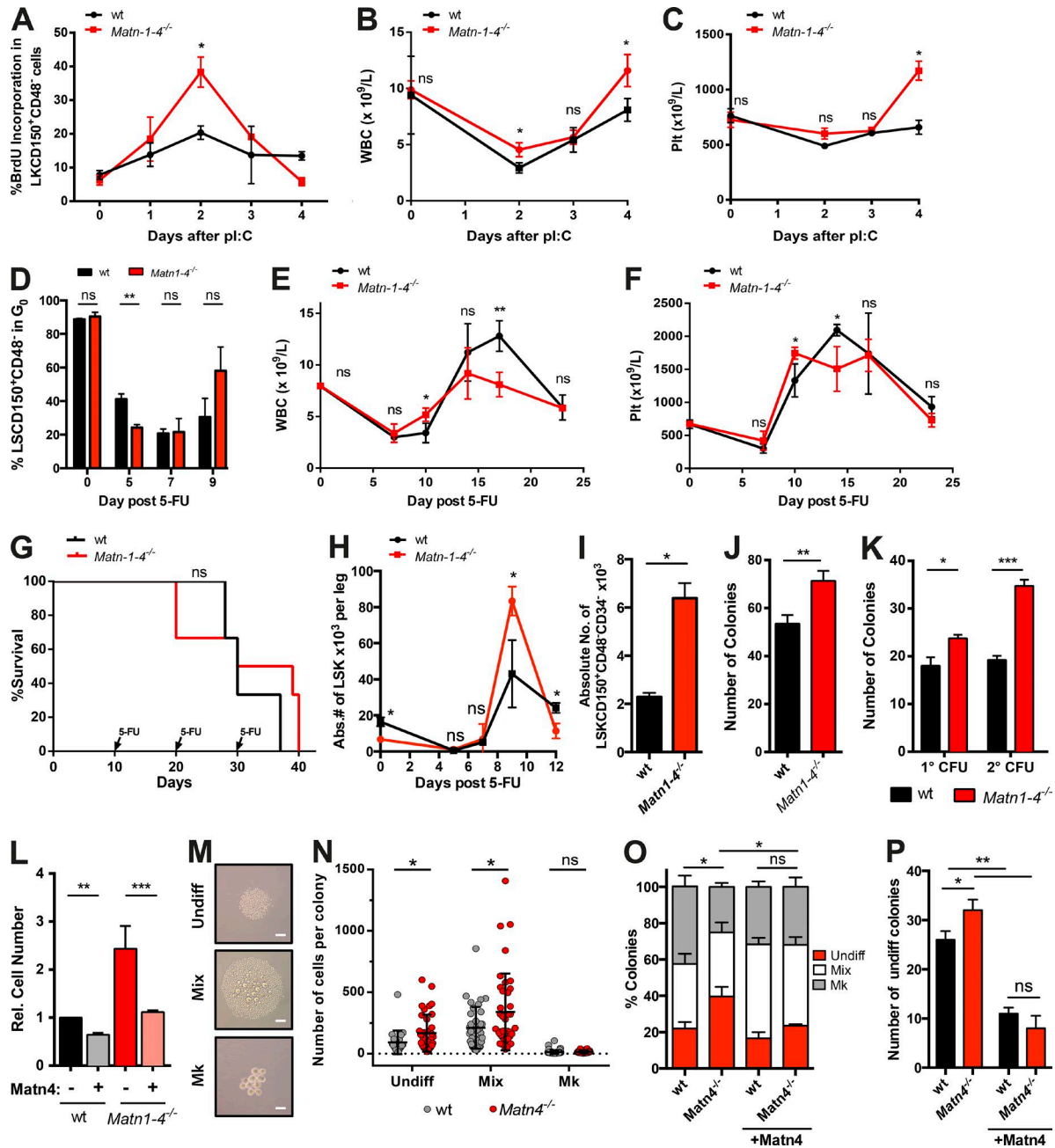
Figure 3. Loss of Matn4 leads to increased HSC proliferation and expansion in response to stress. (A–C) BrdU incorporation (14 h) of HSCs (LKCD150+CD48−; A), WBC counts (B), and platelet (Plt) counts from WT and *Matn1–4−/−* mice treated with PBS (0 d) or pI:C (5 mg/kg at 1, 2, 3, or 4 d). (D) Ki67/Hoechst staining of WT and *Matn1–4−/−* mice was determined 0, 5, 7, or 9 d after PBS or 150 mg/kg 5-FU treatment. (E and F) WBC counts (E) and platelet counts (F) of WT and *Matn1–4−/−* mice, determined 0, 7, 10, 14, 17, and 24 d after 150 mg/kg 5-FU treatment. (G) Survival curve of WT and *Matn1–4−/−* mice treated with 150 mg/kg 5-FU every 10 d. Injection time points are indicated by arrows. $n = 6$ mice/group of two independent experiments. (H) Absolute number (Abs.#) of LSKs per leg 0, 5, 7, and 9 d after 150 mg/kg 5-FU treatment in WT and *Matn1–4−/−* mice. (I) Absolute numbers of WT and *Matn1–4−/−* LT-HSCs (LSKCD150+CD48−CD34−) per two femurs 9 d after 150 mg/kg 5-FU treatment. (J) On day 9 after 5-FU treatment, 2,000 sorted WT and *Matn1–4−/−* LSKs were seeded in CFU assay. The number of colonies was quantified on day 7. (K) WT and *Matn1–4−/−* LSKs were seeded in CFU assay. The number of colonies was quantified on day 7 (1°CFU), reseeded for 2°CFU, and quantified again on day 7. (L) Fold increase in WT and *Matn1–4−/−* cell count of the 1°CFU with or without 100 ng/ml recombinant Matn4 at day 7. Rel., relative. (M–P) Individual WT or *Matn4−/−* HSCs (LSKCD150+CD48−) were sorted into culture medium with or without 100 ng/ml recombinant Matn4. Colony size and types were determined on day 7 using microscopy imaging. Mk, megakaryocytes; Undiff, Undifferentiated. (M) Representative images of each colony type. Bars, 50 µm. (N) Number of cells per colony. (O) Percentage of colony types generated. (P) Number of undifferentiated colonies generated. (A–F and H–P) $n = 3$ mice/group. (A–P) Unless otherwise indicated, unpaired Student's *t* test analysis was performed on three independent experiments for experiments. *, P < 0.05; **, P < 0.01; ***, P < 0.001. Data are mean ± SEM.
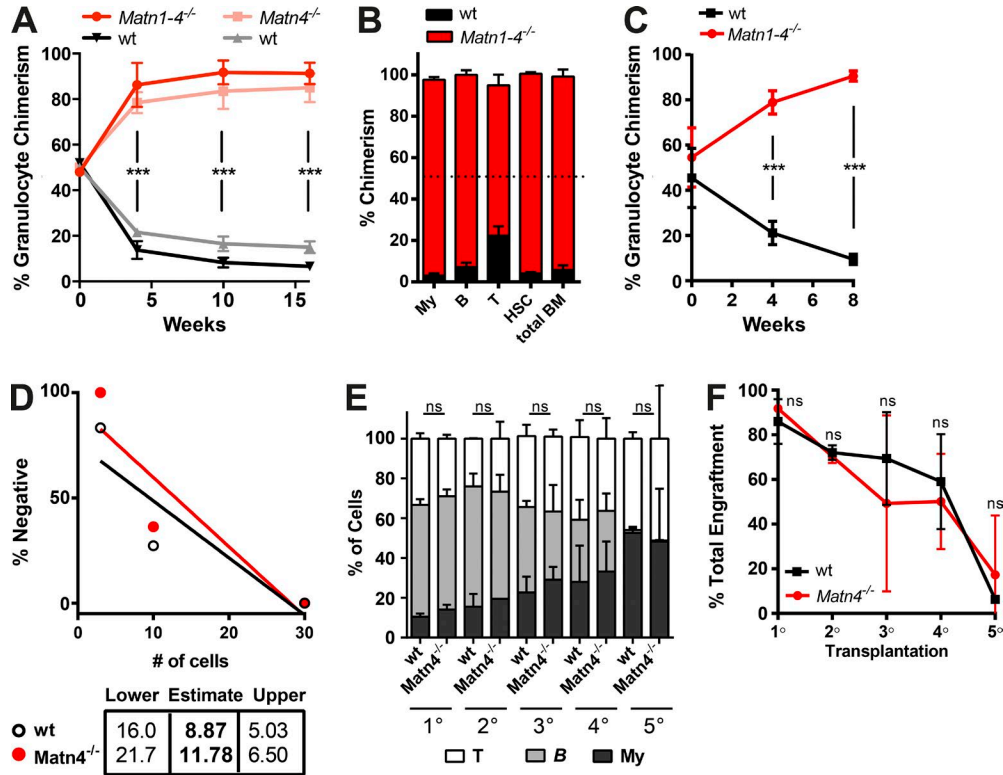
Figure 4. **Matn4–deficient HSCs show improved long–term repopulation capacity.** (A) Blood granulocyte (Gr1+CD11b+) chimerism of WT CD45.1/ *Matn4−/−* or WT CD45.1/*Matn1–4−/−* 50:50 chimeras, determined 0, 4, 10, and 16 wk after transplant. (B) BM chimerism of myeloid (CD11b+Gr-1+), B (B220+), and T cells (CD4+CD8+), HSCs (LSKCD150+CD48−), and whole BM of WT CD45.1/*Matn1–4−/−* 50:50 chimeras 16 wk after transplant. B, B cells; My, myeloid; T, T cells. (C) Blood granulocyte (Gr1+CD11b+) chimerism of secondary WT CD45.1/*Matn1–4−/−* 50:50 chimeras, determined 0, 4, 8, and 20 wk after transplant. (A–C) *n* = 6 mice/group. Unpaired Student's *t* test analysis was performed on three independent experiments. ***, P < 0.001. Data are mean ± SD. (D) 3, 10, or 30 sorted WT CD45.1/2 and *Matn-4−/−* LT-HSCs (LSKCD150+CD48−) were transplanted into lethally irradiated recipients, and engraftment was checked at 8 and 12 wk. The number of HSCs was determined using the ELDA software. Two independent experiments and 3–6 mice/group are shown. (E) Serial transplantations of 100% BM of four individual WT littermate or *Matn4−/−* mice, retransplanted every ≥16 wk into new lethally irradiated recipients. Blood chimerism was analyzed 12–14 wk after transplant. (F) Percent engraftment of WT littermate or *Matn4−/−* BM cells harvested from quaternary chimeras 16 wk after transplant. (E and F) *n* = 4 mice/group. Unpaired Student's *t* test analysis was performed on four biological replicates. ***, P < 0.001. Data are mean ± SEM.

Because KO HSCs proliferate more upon stress, we evaluated their long-term reconstitution capacity. Serial transplantation of 100% *Matn4−/−* or WT littermate BM showed a similar multilineage engraftment (Fig. 4 E) as well as the gradual decrease in reconstitution capacity (Fig. 4 F). Thus, the transient increase in proliferation upon stress observed in Matn-deficient HSCs does not lead to premature exhaustion.

Down-regulation of CXCR4 expression increases proliferation and expansion of *Matn4−/−* HSCs upon stress

To gain insight into the molecular mechanism through which deletion of Matn4 affects HSC function under stress, transcriptional profiling of WT (CD45.1/2) and *Matn4−/−* HSCs was performed 4 wk after competitive transplantation (Fig. 5 A). The overall expression profile of WT and *Matn4−/−* HSCs showed a high correlation. Among the few differentially expressed genes was CXCR4, whereas other known Matn target genes such as collagen X and BMP2 remained un-

changed (Fig. 5, A and B). Furthermore, gene set enrichment analysis revealed transcripts involved in the MAPK signaling pathway and GTPase regulatory activity to be decreased in *Matn4−/−* HSCs (Fig. 5 C), pathways described downstream of CXCR4 (Busillo and Benovic, 2007). It is important to note that CXCR4 levels were equal under homeostasis and only reduced by 50% in transplanted *Matn4−/−* HSCs compared with WT HSCs (Fig. 5 D). The homing capacity of Matn-deficient HSCs was not impaired, indicating that the CXCR4 down-regulation occurred after HSCs homed to the BM (Fig. 5, E and F). Furthermore, no increased mobilization of HSCs could be detected in *Matn1–4−/−* mice in the baseline and upon stress (Fig. 5, G and H), suggesting that *Matn1–4−/−* HSCs are effectively retained within the BM. CXCR4 and its ligand CXCL12 are not only crucial players in HSC homing and migration, but also have been shown to induce HSC cell cycle arrest in homeostasis and upon 5-FU treatment (Sugiyama et al., 2006; Nie et al., 2008;

1966

Matrilin-4 regulates HSC stress response via CXCR4 | Uckelmann et al.

McDermott et al., 2015). Indeed, inhibition of CXCR4 signaling in WT (CD45.1/2) mice by AMD3100 treatment (Broxmeyer et al., 2005) led to increased proliferation of WT HSCs in response to 5-FU and pI:C stress, mimicking the phenotype of $Matn4^{-/-}$ mice (Fig. 5 I). Furthermore, when WT CD45.1/2/$Matn4^{-/-}$ 50:50% chimeras were treated with AMD3100, leading to the reduction of CXCR4 signaling in WT CD45.1/2 HSCs, the proliferative advantage of $Matn4^{-/-}$ initially mediated by differences in CXCR4 expression was rescued (Fig. 5 J). Blood chimerism stayed at 50% 4 wk after transplant and remained significantly lower than in the untreated chimeras, even after discontinuation of the AMD3100 treatment (Fig. 5 J). To further confirm the role of CXCR4, $Matn4^{-/-}$ LSK cells overexpressing CXCR4 were competitively transplanted, and $Matn4^{-/-}$ chimerism remained at ∼50% up to 12 wk after transplant (Fig. 5 K). When CXCR4 was overexpressed in both WT (CD45.1/2) and $Matn4^{-/-}$ cells, we again observed a growth advantage of the $Matn4^{-/-}$ HSCs, indicating that the difference in endogenous CXCR4 levels is still sufficient to provide a competitive advantage. However, we cannot exclude that additional factors are involved in generating a proliferative advantage in Matn-deficient HSCs. Overall, our data show that CXCR4 signaling is an important factor in limiting the proliferation of HSCs in response to different stress stimuli of HSCs in general and establishing the competitive growth advantage of HSCs lacking Matn4 (Fig. 5 L).

In summary, we have uncovered a novel link between ECM component Matn4 and CXCR4 signaling, regulating HSC proliferation and expansion in response to inflammatory stress, chemotherapy, and transplantation. Under homeostasis, high expression of Matn4 in HSCs confers a resistance to stress stimuli. In situations of acute stress, Matn4 is down-regulated to release this protection to allow HSCs to efficiently replenish the blood system. Interestingly, in vitro recombinant Matn4 can act as a cytokine with growth inhibitory effects. However, in mixed chimeras, Matn4 produced by WT BM cannot rescue $Matn4^{-/-}$ HSC expansion, suggesting that Matn4 acts locally on HSCs through an autocrine or even intracellular mechanism. Because reduced CXCR4 levels in $Matn4^{-/-}$ HSCs led to improved stress recovery and reconstitution upon transplantations, it will be of great interest to investigate whether the CXCR4 antagonist AMD3100 could be used to improve the recovery of patients from hematopoietic stress such as myelosuppressive chemotherapy and transplantation.

MATERIALS AND METHODS
Animals
Mice were maintained in individually ventilated cages in the DKFZ animal facility. Female 8–12-wk-old mice were used throughout the study. As controls, C57BL/6 (WT) or B6.SJL-Ptprc[a] Pepc[b]/BoyJ (WT CD45.1) mice purchased from Envigo or Charles River, respectively, were used as indicated. Control WT CD45.1/2 mice were obtained by crossing

WT CD45.2 and WT CD45.1 mice. To generate $Matn4^{-/-}$ mice, a neomycin-thymidine kinase–containing selection cassette floxed with loxP sites was introduced into the second intron and a single loxP site into the third intron of the mouse $Matn4$ gene. The targeting construct was electroporated into R1 embryonic stem (ES) cells and subjected to G418 selection. One homologous recombinant ES cell clone identified by Southern blotting was transiently transfected with Cre recombinase followed by selection against the thymidine kinase gene with Fialuridine. ES cells carrying the null allele, which lacks exon 1 with the translation initiation codon as well as the selection cassette and only contains one loxP site in the second intron, were used to establish the $Matn4^{-/-}$ line. $Matn4^{-/-}$ mice were backcrossed more than eight times on a C57BL/6 background. Quadruple KO mice deficient for all Matn family members ($Matn1$–$4^{-/-}$) were generated by intercrossing individual $Matn4$-, $Matn3$ (Ko et al., 2004)-, $Matn2$ (Mátés et al., 2004)-, and $Matn1$ (Aszódi et al., 1999)–mutant lines and backcrossed to a >90% C57BL/6 background. $Ifnar^{-/-}$ (Müller et al., 1994) and $Stat1^{-/-}$ (Durbin et al., 1996) have been described previously. All animal protocols were approved by the Animal Care and Use Committees of the German Regierungspräsidium Karlsruhe für Tierschutz und Arzneimittelüberwachung.

In vivo treatments
Mice were injected i.p. with PBS; 5 mg/kg pI:C (InvivoGen), 5×10^6 U/kg recombinant mouse IFN-α (Miltenyi Biotec), 0.25 mg/kg LPS (*Escherichia coli* 0111:B4; Sigma-Aldrich), and 150 mg/kg 5-FU; or s.c. with 5 mg/kg AMD3100 (Sigma-Aldrich). Chimeras were treated with AMD3100 starting 2 d after transplant to allow homing and then treated three times per week.

Isolation of BM cells and peripheral blood (PB)
Mice were sacrificed, and tibiae, femurs, sternum, coxae, and vertebral columns were crushed in RPMI-1640 medium (Sigma-Aldrich) supplemented with 2% FCS. For cell sorting, lineage depletion was performed by incubating BM cells with rat monoclonal antibodies targeting CD4 (GK1.5), CD8a (53.6.7), CD11b (M1/70), B220 (RA3-6B2), Gr-1 (RB6.8C5), and Ter119 (Ter119). Subsequently, cells were washed, and lin^+ cells were removed using magnetic beads (Dynabeads; Invitrogen). For analysis of PB, four to five drops of blood were collected from the vena facialis into an EDTA-coated tube. Blood cells were analyzed using a hematology system (Hemavet 950; Drew Scientific). For FACS analysis, erythrocytes were lysed with 1 ml ammonium-chloride-potassium lysing buffer.

Flow cytometry and cell sorting
BM cells were incubated with antibodies for 30 min on ice. BM cells were stained for HSCs and progenitors using antibodies CD4 (GK1.5), CD8 (53-6.7), CD11b (M1/70), Gr-1 (RB6-8C5), B220 (RA3-6B2), and TER119 (TER119);
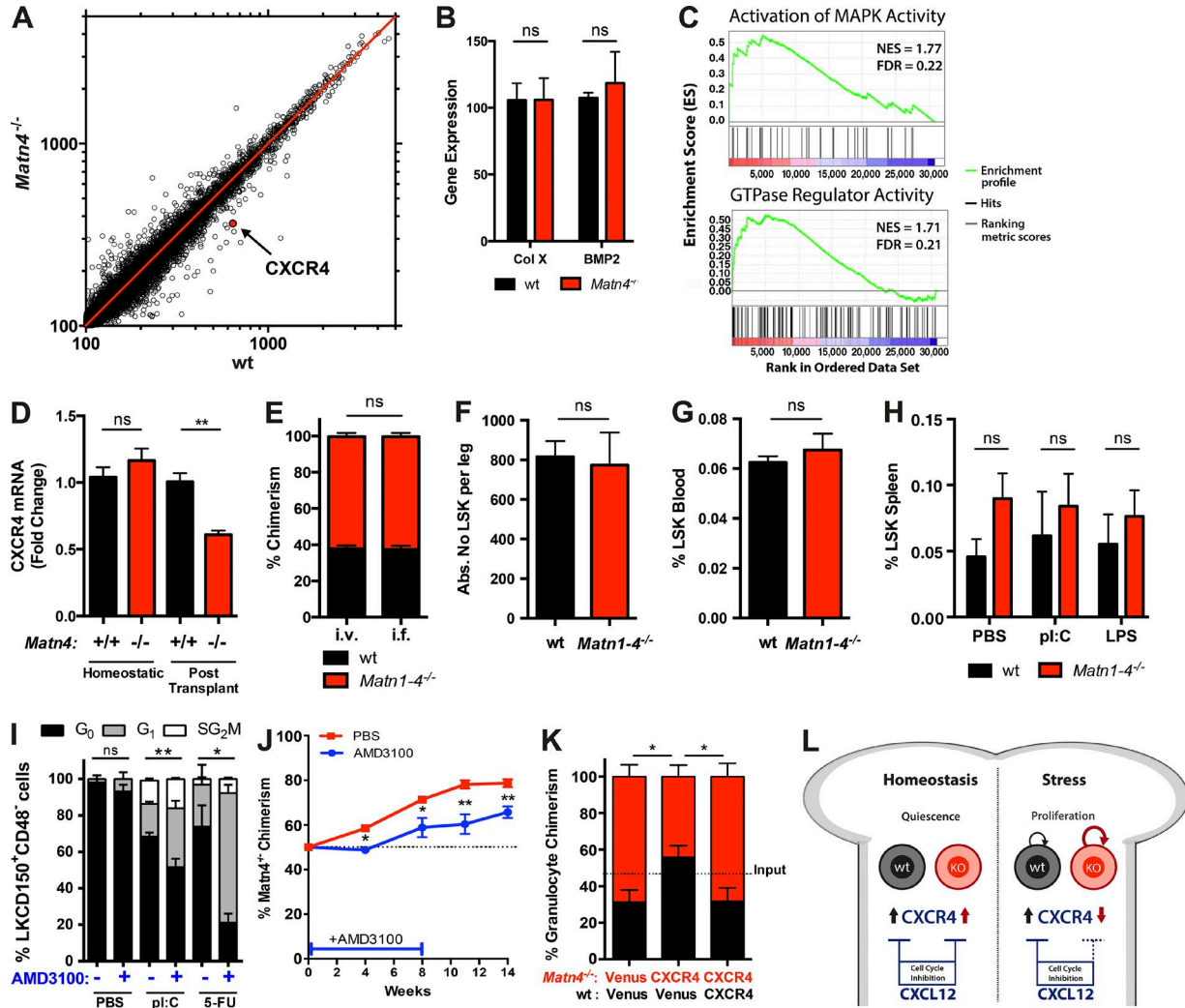
Figure 5. Proliferative advantage of Matn-4⁻/⁻ HSCs is mediated by down-regulation of CXCR4. (A) Scatterplot showing changes in mean mRNA expression levels (microarray) of three WT CD45.1/2 and three *Matn4⁻/⁻* HSCs (LSKCD150⁺CD48⁺) isolated from WT CD45.1/2/ *Matn4⁻/⁻* 50:50 chimeras 4 wk after transplant. CXCR4 is marked in red. (B) Collagen X (Col X) and BPM2 mRNA expression levels of sorted HSCs (LSKCD150⁺CD48⁻) from WT CD45.1/2/*Matn4⁻/⁻* 50:50 chimeras isolated 4 wk after transplant, derived from microarray analysis. Unpaired Student's *t* test analysis was performed on three biological replicates. Data are mean ± SD. (C) Gene set enrichment analysis of activation of MAPK activity and GTPase regulatory activity using WT and *Matn4⁻/⁻* microarray gene expression data. Positively (red) and negatively (blue) regulated genes are shown (P < 0.05). FDR, false discovery rate; NES, normalized enrichment score. (D) Fold change of CXCR4 mRNA expression validated by qRT-PCR of sorted HSCs (LSKCD150⁺CD48⁻) from WT CD45.1/2/ *Matn4⁻/⁻* 50:50 chimeras (after transplant) or untransplanted WT CD45.1/2 and *Matn4⁻/⁻* mice (homeostatic), determined by qRT-PCR. (E) BM of WT CD45.1/2 and *Matn1-4⁻/⁻* was transplanted 50:50 i.v. or intrafemurally (i.f.). Blood granulocyte (Gr1⁺CD11b⁺) chimerism was checked 4 wk after transplant. (F) WT CD45.1/2 and *Matn1-4⁻/⁻* BM was transplanted 50:50 i.v. The absolute number (Abs. No) of LSKs per leg was determined by FACS 16 h after transplant. (G) Quantification of mobilized LSKs in the blood of untreated WT and Matn1-4⁻/⁻ mice. (H) Quantification of mobilized LSKs in the spleen of untreated, pl:C-treated, or LPS-treated WT and Matn1-4⁻/⁻ mice. (I) Ki67/Hoechst staining of WT HSCs (LSCD150⁺CD48⁻CD34⁻) after 150 mg/kg 5-FU (9 d) or 5 mg/kg pl:C treatment (2 d) and/or 5 mg/kg AMD3100 (every second day) treatment. (J) WT CD45.1/2/*Matn4⁻/⁻* 50:50 chimeras were treated with 5 mg/kg AMD3100 for 8 wk (three times per week). Blood granulocyte (Gr1⁺CD11b⁺) chimerism was determined 0, 4, 8, 11, and 14 wk after transplant. *n* = 6 mice/group. (K) 50:50 chimeras were generated using WT CD45.1/2 (black) or *Matn4⁻/⁻* (red) LSKs overexpressing CXCR4 or a Venus control. Blood granulocyte (Gr1⁺CD11b⁺) chimerism was determined 12 wk after transplant. (L) Schematic overview: under homeostatic conditions, WT and *Matn4⁻/⁻* HSCs express equal levels of CXCR4. Under stress conditions, *Matn4⁻/⁻* HSCs have reduced CXCR4 expression, resulting in a decreased inhibition of their cell cycle during acute stress. (A, B, D–I, and K) *n* = 3 mice/group. (D–J) Unpaired Student's *t* test analysis was performed on three independent experiments. *, P < 0.05; **, P < 0.01. Data are mean ± SEM.

CD16/32 (93), CD41 (MW Reg 30), and CD105 (MJ7/18); and cKit (2B8), Sca-1 (D7), CD150 (TC15-12F12.1), CD48 (HM48-1), and CD34 (RAM34; eBioscience). When comparing untreated to pI:C/LPS-treated HSCs, Sca-1 was excluded from the gating because of its strong up–regulation. After 5-FU treatment, c-Kit was excluded from the HSC gating scheme, as its expression on HSCs is lost during 5-FU recovery. Cells were analyzed using an LSRII or LSR Fortessa flow cytometer (BD). Data were analyzed using FlowJo software (Tree Star). For FACS sorting, FACSAria I, II, and III cell sorters were used (BD).

Cell cycle analysis
BM cells were stained with surface markers as described under the Flow cytometry and cell sorting section, fixed using Cytox/Cytoperm buffer (BD), and stained with Ki67 antibody overnight at 4°C. Hoechst 33342 stain (Molecular Probes) was added at 25 µg/ml before FACS analysis. For the BrdU incorporation assay, mice were injected i.p. with 18 mg/kg BrdU (Sigma–Aldrich) 14 h before harvesting the BM. For BrdU staining, the BD BrdU Flow kit was used.

BM transplantations
3×10^6 cells were diluted in 100–200 µl PBS and i.v. injected into lethally irradiated (2×500 rad) mice. For mixed BM chimeras, 1.5×10^6 BM cells of each genotype were mixed before i.v. injection. For 2° chimeras, WT and KO BM of 1° 50:50 chimeras at week 16 were mixed 1:1 and transplanted into lethally irradiated recipients. Mice were kept on antibiotics (Cotrim) for 3 wk after transplant. Blood chimerism was monitored monthly.

Limiting dilution assay
3, 10, and 30 sorted WT CD45.1/2 or $Matn4^{-/-}$ LT-HSCs were transplanted i.v. together with 2×10^5 supportive BM cells into lethally irradiated WT CD45.1 recipients. PB was analyzed for myeloid and lymphoid reconstitution at 8 and 12 wk, and HSC engraftment in BM was analyzed at 14 wk. Mice for which engraftment was <1% were considered non-engrafted and were not taken into account for calculation of stem cell frequencies. Calculation of stem cell frequencies and statistics was performed using ELDA software.

Homing assays
3×10^6 BM cells were injected either i.v. or intrafemurally into lethally irradiated recipients, and blood chimerism was monitored monthly. Alternatively, 50×10^6 BM cells per mouse were transplanted i.v., femurs were harvested after 16 h, and the number of LSKs in the BM was analyzed by FACS.

Generation of CXCR4 retrovirus
A retroviral overexpression system for CXCR4 was generated using the SF91 retroviral vector (Milsom et al., 2009). Viral supernatants were generated from Phoenix cells (ATCC). Cells were transfected with either SF-CXCR4 or SF-Venus

using calcium phosphate transfection (Invitrogen). Retroviral supernatant was harvested 48 h after transfection, concentrated by ultracentrifugation, and stored at −80°C until use.

In vitro culture
After FACS sorting, cells were cultured in Stem-Pro34 medium (Invitrogen) supplemented with 1% L-glutamine, 1% penicillin/streptomycin, 26% N-2 Supplement (Invitrogen), 50 ng/ml Flt3, 50 ng/ml mouse thrombopoietin, and 50 ng/ml mouse stem cell factor (R&D Systems). Cells were cultured at 37°C and 5% CO_2.

Transduction of mouse LSK cells
LSK cells were cultured in Stem-pro34 medium for 48 h and transferred to nontissue culture–coated plates (BD) precoated with fibronectin CH296 fragment (Takara Bio Inc.) at 4 µg/cm^2. LSK cells were seeded with concentrated retroviral supernatant at a multiplicity of infection of 4. 36 h later, cells were harvested, and live Venus^{+} cells were sorted.

Immunofluorescence
Sorted HSCs were added onto Polysine slides and incubated at room temperature for 15 min. Cells were fixed with Cytox/Cytoperm buffer (BD) for 10 min, blocked with 15% goat serum (Dako), and incubated with a rabbit polyclonal antibody against Matn4 (ab106379; Abcam) overnight at 4°C. Subsequently, slides were incubated for 1 h at 4°C with anti–rabbit IgG-F(AB)2-DyLight649 (Jackson ImmunoResearch Laboratories, Inc.) and mounted with ProLong Gold mounting medium containing DAPI (Invitrogen). Slides were analyzed on a cell observer (ZEISS) and documented with an AxioCam HR camera (ZEISS).

Colony forming assay
500 LSK cells were plated in 1 ml of Methocult 3434 (STEMCELL Technologies) supplemented with PBS or 100 ng/ml recombinant Matn4 (R&D Systems). Colonies consisting of >40 cells were counted using an inverted microscope after 7 d.

Microarray
4 wk after transplant, HSCs were sorted, and RNA was isolated using an RNA isolation kit (Arcturus PicoPure; Applied Biosystems). 2.5 ng RNA was used for hybridization onto the Mouse Sentrix–6 Bead-Chip array (Illumina). Microarray data were deposited in NCBI's Gene Expression Omnibus under accession no. GSE72814.

Quantitative real–time PCR (qRT–PCR)
Cells were FACS sorted into 50–100 µl of extraction buffer (Arcturus PicoPure kit), and RNA was isolated with the PicoPure RNA isolation kit (Arcturus). RNA was reverse transcribed with the SuperScript VILO cDNA synthesis kit (Invitrogen). For qRT-PCR, the ViiA 7 Real-Time PCR system (Applied Biosystems) was used with 384–well plates. Sdha was used as the housekeeping gene for normalization. Rela-

tive gene expression was calculated by the comparative ΔΔ cycle threshold method. The primers used in the real-time PCR were: Matn4 forward, 5′-TTAGCACCATGACGC ACCT-3′; reverse, 5′-GGACTCCGAAGCTCTGTCC-3′; CXCR4 forward, 5′-GACTGGCATAGTCGGCAATG-3′; reverse, 5′-AGAAGGGGAGTGTGATGACAAA-3′; SDHA forward, 5′-AAGTTGAGATTTGCCGATGG-3′; and reverse, 5′-TGGTTCTGCATCGACTTCTG-3′.

Statistical analysis

For statistical analysis and graphical representation of data, Prism 6.0 (GraphPad Software) was used. Statistical analysis was performed using two–tailed unpaired Student's *t* tests. All data are expressed as mean ± SEM unless otherwise indicated. Statistical significance is indicated by *, P < 0.05; **, P < 0.01; and ***, P < 0.001.

Online supplemental material

Fig. S1 shows the gating scheme used to gate on LSK cells after 0, 5, 9, and 12 d of 5-FU treatment. Online supplemental material is available at http://www.jem.org/cgi/content/full/jem.20151713/DC1.

REFERENCES

Aszódi, A., J.F. Bateman, E. Hirsch, M. Baranyi, E.B. Hunziker, N. Hauser, Z. Bösze, and R. Fässler. 1999. Normal skeletal development of mice lacking matrilin 1: redundant function of matrilins in cartilage? *Mol. Cell. Biol.* 19:7841–7845. http://dx.doi.org/10.1128/MCB.19.11.7841

Baldridge, M.T., K.Y. King, N.C. Boles, D.C. Weksberg, and M.A. Goodell. 2010. Quiescent haematopoietic stem cells are activated by IFN-γ in response to chronic infection. *Nature.* 465:793–797. http://dx.doi.org/10.1038/nature09135

Broxmeyer, H.E., C.M. Orschell, D.W. Clapp, G. Hangoc, S. Cooper, P.A. Plett, W.C. Liles, X. Li, B. Graham-Evans, T.B. Campbell, et al. 2005. Rapid mobilization of murine and human hematopoietic stem and progenitor cells with AMD3100, a CXCR4 antagonist. *J. Exp. Med.* 201:1307–1318. http://dx.doi.org/10.1084/jem.20041385

Busillo, J.M., and J.L. Benovic. 2007. Regulation of CXCR4 signaling. *Biochim. Biophys. Acta.* 1768:952–963. http://dx.doi.org/10.1016/j.bbamem.2006.11.002

Deák, F., R. Wagener, I. Kiss, and M. Paulsson. 1999. The matrilins: a novel family of oligomeric extracellular matrix proteins. *Matrix Biol.* 18:55–64. http://dx.doi.org/10.1016/S0945-053X(98)00006-7

Durbin, J.E., R. Hackenmiller, M.C. Simon, and D.E. Levy. 1996. Targeted disruption of the mouse *Stat1* gene results in compromised innate immunity to viral disease. *Cell.* 84:443–450. http://dx.doi.org/10.1016/S0092-8674(00)81289-1

Ellis, S.J., and G. Tanentzapf. 2010. Integrin-mediated adhesion and stem-cell-niche interactions. *Cell Tissue Res.* 339:121–130. http://dx.doi.org/10.1007/s00441-009-0828-4

Essers, M.A., S. Offner, W.E. Blanco-Bose, Z. Waibler, U. Kalinke, M.A. Duchosal, and A. Trumpp. 2009. IFNα activates dormant haematopoietic stem cells in vivo. *Nature.* 458:904–908. http://dx.doi.org/10.1038/nature07815

Heissig, B., K. Hattori, S. Dias, M. Friedrich, B. Ferris, N.R. Hackett, R.G. Crystal, P. Besmer, D. Lyden, M.A.S. Moore, et al. 2002. Recruitment of stem and progenitor cells from the bone marrow niche requires MMP-9 mediated release of kit-ligand. *Cell.* 109:625–637. http://dx.doi.org/10.1016/S0092-8674(02)00754-7

Itkin, T., and T. Lapidot. 2011. SDF-1 keeps HSC quiescent at home. *Blood.* 117:373–374. http://dx.doi.org/10.1182/blood-2010-09-307843

Katayama, Y., M. Battista, W.-M. Kao, A. Hidalgo, A.J. Peired, S.A. Thomas, and P.S. Frenette. 2006. Signals from the sympathetic nervous system regulate hematopoietic stem cell egress from bone marrow. *Cell.* 124:407–421. http://dx.doi.org/10.1016/j.cell.2005.10.041

Klatt, A.R., D.P. Nitsche, B. Kobbe, M. Macht, M. Paulsson, and R. Wagener. 2001. Molecular structure, processing, and tissue distribution of matrilin-4. *J. Biol. Chem.* 276:17267–17275. http://dx.doi.org/10.1074/jbc.M100587200

Klatt, A.R., A.-K.A. Becker, C.D. Neacsu, M. Paulsson, and R. Wagener. 2011. The matrilins: modulators of extracellular matrix assembly. *Int. J. Biochem. Cell Biol.* 43:320–330. http://dx.doi.org/10.1016/j.biocel.2010.12.010

Klein, G. 1995. The extracellular matrix of the hematopoietic microenvironment. *Experientia.* 51:914–926. http://dx.doi.org/10.1007/BF01921741

Ko, Y., B. Kobbe, C. Nicolae, N. Miosge, M. Paulsson, R. Wagener, and A. Aszódi. 2004. Matrilin-3 is dispensable for mouse skeletal growth and development. *Mol. Cell. Biol.* 24:1691–1699. http://dx.doi.org/10.1128/MCB.24.4.1691-1699.2004

Mann, H.H., G. Sengle, J.M. Gebauer, J.A. Eble, M. Paulsson, and R. Wagener. 2007. Matrilins mediate weak cell attachment without promoting focal adhesion formation. *Matrix Biol.* 26:167–174. http://dx.doi.org/10.1016/j.matbio.2006.10.010

Mátés, L., C. Nicolae, M. Mörgelin, F. Deák, I. Kiss, and A. Aszódi. 2004. Mice lacking the extracellular matrix adaptor protein matrilin-2 develop without obvious abnormalities. *Matrix Biol.* 23:195–204. http://dx.doi.org/10.1016/j.matbio.2004.05.003

McDermott, D.H., J.-L. Gao, Q. Liu, M. Siwicki, C. Martens, P. Jacobs, D. Velez, E. Yim, C.R. Bryke, N. Hsu, et al. 2015. Chromothriptic cure of WHIM syndrome. *Cell.* 160:686–699. http://dx.doi.org/10.1016/j.cell.2015.01.014

Milsom, M.D., B. Schiedlmeier, J. Bailey, M.-O. Kim, D. Li, M. Jansen, A.M. Ali, M. Kirby, C. Baum, L.J. Fairbairn, and D.A. Williams. 2009. Ectopic HOXB4 overcomes the inhibitory effect of tumor necrosis factor-α on Fanconi anemia hematopoietic stem and progenitor cells. *Blood.* 113:5111–5120. http://dx.doi.org/10.1182/blood-2008-09-180224

Müller, U., U. Steinhoff, L.F. Reis, S. Hemmi, J. Pavlovic, R.M. Zinkernagel, and M. Aguet. 1994. Functional role of type I and type II interferons in antiviral defense. *Science.* 264:1918–1921. http://dx.doi.org/10.1126/science.8009221

Nicolae, C., Y.-P. Ko, N. Miosge, A. Niehoff, D. Studer, L. Enggist, E.B. Hunziker, M. Paulsson, R. Wagener, and A. Aszodi. 2007. Abnormal collagen fibrils in cartilage of matrilin-1/matrilin-3-deficient mice. *J. Biol. Chem.* 282:22163–22175. http://dx.doi.org/10.1074/jbc.M610994200

Nie, Y., Y.-C. Han, and Y.-R. Zou. 2008. CXCR4 is required for the quiescence of primitive hematopoietic cells. *J. Exp. Med.* 205:777–783. http://dx.doi.org/10.1084/jem.20072513

Orkin, S.H., and L.I. Zon. 2008. Hematopoiesis: an evolving paradigm for stem cell biology. *Cell.* 132:631–644. http://dx.doi.org/10.1016/j.cell.2008.01.025

Sato, T., N. Onai, H. Yoshihara, F. Arai, T. Suda, and T. Ohteki. 2009. Interferon regulatory factor-2 protects quiescent hematopoietic stem cells from type I interferon-dependent exhaustion. *Nat. Med.* 15:696–700. http://dx.doi.org/10.1038/nm.1973

Scadden, D.T. 2014. Nice neighborhood: emerging concepts of the stem cell niche. *Cell.* 157:41–50. http://dx.doi.org/10.1016/j.cell.2014.02.013

Sugiyama, T., H. Kohara, M. Noda, and T. Nagasawa. 2006. Maintenance of the hematopoietic stem cell pool by CXCL12-CXCR4 chemokine signaling in bone marrow stromal cell niches. *Immunity.* 25:977–988. http://dx.doi.org/10.1016/j.immuni.2006.10.016

Tzeng, Y.-S., H. Li, Y.-L. Kang, W.-C. Chen, W.-C. Cheng, and D.-M. Lai. 2011. Loss of Cxcl12/Sdf-1 in adult mice decreases the quiescent state of hematopoietic stem/progenitor cells and alters the pattern of hematopoietic regeneration after myelosuppression. *Blood.* 117:429–439. http://dx.doi.org/10.1182/blood-2010-01-266833

Walter, D., A. Lier, A. Geiselhart, F.B. Thalheimer, S. Huntscha, M.C. Sobotta, B. Moehrle, D. Brocks, I. Bayindir, P. Kaschutnig, et al. 2015. Exit from dormancy provokes DNA-damage–induced attrition in haematopoietic stem cells. *Nature.* 520:549–552. http://dx.doi.org/10.1038/nature14131

Xun, C.Q., J.S. Thompson, C.D. Jennings, S.A. Brown, and M.B. Widmer. 1994. Effect of total body irradiation, busulfan-cyclophosphamide, or cyclophosphamide conditioning on inflammatory cytokine release and development of acute and chronic graft-versus-host disease in H-2-incompatible transplanted SCID mice. *Blood.* 83:2360–2367.